

# A numerical strategy for efficient modeling of the equatorial wave guide

Andrew J. Majda\* and Boualem Khouider

Courant Institute of Mathematical Sciences, New York University, New York, NY 10012

Contributed by Andrew J. Majda, December 7, 2000

Convection in the tropics is observed to involve a wide-ranging hierarchy of scales from a few kilometers to the planetary scales and also has a profound impact on short-term climate. The mechanisms responsible for this behavior present a major unsolved problem. A promising emerging approach to address these issues is cloud-resolving modeling. Here a family of numerical models is introduced specifically to model the feedback of small-scale deep convection on tropical planetary waves and tropical circulation in a highly efficient manner compatible with the approach through cloud-resolving modeling. Such a procedure is also useful for theoretical purposes. The basic idea in the approach is to use low-order truncation in the meridional direction through Gauss–Hermite quadrature projected onto a simple discrete radiation condition. In this fashion, the cloud-resolving modeling of equatorially trapped planetary waves reduces to the solution of a small number of purely zonal two-dimensional wave systems along a few judiciously chosen meridional layers that are coupled only by some additional source terms. The approach is analyzed in detail with full mathematical rigor for linearized equatorial primitive equations with source terms.

Convection in the tropics has a profound impact on short-term climate. Observational data indicate that tropical deep convection is organized on a hierarchy of scales ranging from cumulus clouds over a few kilometers to interseasonal oscillations over planetary scales of order 40,000 km (1–3). The mechanisms for this behavior present a major unsolved problem, despite the fact that there has been extensive research over the last few decades on these topics through parameterization of convection in general circulation models (4) as well as theory (refs. 5 and 6 and refs. therein). A particularly promising emerging approach to address these issues is cloud-resolving modeling (CRM), where idealized highly resolved two-dimensional simulations of clouds are coupled to larger-scale dynamics in a variety of ways (7–9), utilizing massively parallel computer architecture. Nevertheless, only very crude resolution of the large-scale interaction is possible with the current generation of computers. Here a hierarchy of numerical models is introduced specifically to model the feedback of small-scale deep convection on the tropical planetary waves and tropical circulation in a highly efficient manner compatible with the CRM approach. Besides its efficiency, this numerical strategy also makes a direct link with many of the observed larger-scale patterns in the equatorial wave guide such as Kelvin, Yanai, and equatorial Rossby waves (3, 10, 11), so that observations, theory, and CRM simulations can be compared in an interactive fashion.

The basic idea in the approach is to use low-order truncation in the meridional direction through Hermite polynomials combined with Gauss–Hermite quadrature in a meridional Galerkin approximation projected onto a simple discrete radiation condition. In this fashion, for example, the numerical CRM of equatorially trapped solutions symmetric about the equator at planetary scales reduces to the solution of a small number of purely zonal (i.e., two-dimensional) wave systems along a few judiciously chosen meridional layers that are only locally coupled by using additional source terms. Thus, there is only mild overhead to include the effects of rotation within the tropical wave guide compared with the purely zonal decoupled cloud-resolving models (7–9).

The procedure using meridional truncation is a systematic way to derive reduced models for the equatorial wave guide akin to the familiar well-known strategy of using multilayer models in a vertical truncation of the quasigeostrophic or primitive equations in mid-latitude (11). However, the technical details are quite different and are specifically adapted to the equatorial wave guide. A simplified version of the basic meridional truncation strategy has been introduced recently in ref. 5 for theoretical purposes to study parameterization of convectively coupled tropical waves; the systematic use of low-order Gauss–Hermite quadrature is the key new fact that turns this basic approach into a practical numerical strategy.

The plan for the rest of this paper is the following: first, basic properties of parabolic cylinder functions, Hermite polynomials, and Gauss–Hermite quadrature are reviewed, which are necessary for the remaining developments in the paper. Next, a brief summary of the wave properties of the linearized equatorial primitive equations is presented. Then the basic Galerkin-collocation strategy is presented for a general nonlinear equation having a structure consistent with the equatorial wave guide; this formulation is general enough to include as examples the moist anelastic equations, the primitive equations, and other simplified theoretical nonlinear models for convectively coupled planetary waves with reduced vertical structure. Also the need for a simple discrete radiation condition is demonstrated here. Any cloud-resolving discretization of the  $(x, z)$  equations (7–9) can be implemented easily in the approach. Finally, the meridional truncation strategy is developed for the linearized equatorial primitive equations to provide a fundamental illustrative example of the approach, including both its strengths and shortcomings.

## Parabolic Cylinder Functions, Hermite Polynomials, and Gauss–Hermite Quadrature

The parabolic cylinder functions are given by

$$D_N(\xi) = 2^{-N/2} H_N(\xi/\sqrt{2}) e^{-\xi^2/4},$$

$$H_N(\xi) = (-1)^N e^{\xi^2} \frac{d^N e^{-\xi^2}}{d\xi^N}, \quad N = 0, 1, \dots, \quad [1]$$

where  $H_N(\xi)$  are the Hermite polynomials. An orthonormal basis for  $L^2$  on the line is given by

$$\varphi_N = (N! \sqrt{\pi})^{-1/2} D_N(\sqrt{2}y), \quad \text{so that} \quad \int \varphi_N \varphi_M dy = \delta_{N,M}. \quad [2]$$

The parabolic cylinder functions are the well-known eigenfunctions of the quantum harmonic oscillator (12, 13) and have the following properties associated with the raising and lowering operators of quantum mechanics:

Abbreviation: CRM, cloud-resolving modeling.

\*To whom reprint requests should be addressed. E-mail: jonjon@cims.nyu.edu.

Article published online before print: *Proc. Natl. Acad. Sci. USA*, 10.1073/pnas.041583698.  
Article and publication date are at [www.pnas.org/cgi/doi/10.1073/pnas.041583698](http://www.pnas.org/cgi/doi/10.1073/pnas.041583698)

$$\begin{aligned} \text{with } L_{\pm} &= \frac{d}{dy} \pm y \\ L_{+} \varphi_N(y) &= (2N)^{1/2} \varphi_{N-1}(y) \\ L_{-} \varphi_N(y) &= -(2(N+1))^{1/2} \varphi_{N+1}(y). \end{aligned} \quad [3]$$

Below, the obvious identities are utilized,

$$y = \frac{1}{2}(L_{+} - L_{-}), \quad \frac{d}{dy} = \frac{1}{2}(L_{+} + L_{-}). \quad [4]$$

Next, Gauss–Hermite quadrature is introduced (13, 14). Given the Hermite polynomial,  $H_N(y)$ , let  $y_j, j = 1, \dots, N$ , denote the  $N$  real zeroes

$$H_N(y_j) = 0, \quad j = 1, \dots, N. \quad [5]$$

For a given  $N$ , these points  $y_j$  will define the  $N$ -meridional levels of the truncated model. In Gauss–Hermite quadrature, given  $N$  and the nodes  $y_j, 1 \leq j \leq N$ , there are positive quadrature coefficients,  $\bar{H}_j$ , so that if one introduces the discrete inner product for functions  $f(y), g(y)$  by

$$(f, g)_N = \sum_{j=1}^N f(y_j)g(y_j)\bar{H}_j, \quad [6]$$

then the discrete functions,  $\varphi_l(y_j), \varphi_m(y_j)$  are also a discrete orthonormal basis,

$$(\varphi_l, \varphi_m) = \delta_{l,m} \quad \text{for } m, l < N. \quad [7]$$

Explicit formulas for  $\bar{H}_j$  can be found in refs. 13 and 14. In particular, for a function  $f(y)$ , the  $L^2$ -projection,  $P_N f$ , is defined by

$$P_N f = \sum_{j=0}^{N-1} \tilde{f}_j \varphi_j(y), \quad [8]$$

with  $\tilde{f}_j = \int f \varphi_j dy$ . By combining Eqs. 6, 7, and 8, it follows that if one begins with any function  $f(y)$  satisfying  $P_N f = f$ , then

$$\begin{aligned} P_N f(y_j) &= \sum_{l=0}^{N-1} \tilde{f}_l \varphi_l(y_j), \quad j = 1, \dots, N \\ \tilde{f}_l &= \sum_{j=1}^N f(y_j) \varphi_l(y_j) \bar{H}_j \\ &\stackrel{\text{Def.}}{=} (f, \varphi_l)_N, \quad l = 1, \dots, N. \end{aligned} \quad [9]$$

The formulas in Eq. 9 show that given  $N$ , taking the discrete inner product of the  $\varphi_j$  at the discrete levels  $y_j$  with the quadrature coefficients  $\bar{H}_j$  in the above fashion exactly reproduces the discrete values of all functions  $f(y)$  with  $P_N f = f$ .

### The Equatorial Primitive Equations

An important prototype example to test the numerical strategy developed below is given by the linearized hydrostatic equatorial primitive equations with source terms

$$\begin{aligned} \frac{\partial \vec{v}_H}{\partial t} + y \vec{v}_H^{\perp} &= -\nabla_H P \\ -p_z + B &= 0 \\ \frac{\partial B}{\partial t} + \bar{N}^2 w &= S(x, y, z, t) \\ \text{div}_H \vec{v}_H + w_z &= 0. \end{aligned} \quad [10]$$

Here  $\vec{v}_H = (u(x, y, z, t), v(x, y, z, t))$  is the horizontal velocity field with  $\vec{v}_H^{\perp} = (-v, u)$ ,  $w$  is the vertical velocity, and  $B$  is the buoyancy, with  $\bar{N}$  the constant buoyancy frequency. Rigid lid boundary conditions will be utilized here to mimic dynamics in the troposphere. The model in Eq. 10 already incorporates a number of key features at large scales in a CRM method for the equatorial wave guide (7–9). The CRM approach on the coarse-grained large scales would involve additional nonlinear advection terms in Eq. 10 as well as nonlinear interactive source terms,  $S(x, y, z, t)$ , depending on the cloud-resolving components not given explicitly in Eq. 10 (9). The nonlinear advective terms are treated by the systematic approach in the next section, whereas the source terms require only a separate fractional step in the numerical procedure (9). Thus, the model in Eq. 10 captures a significant number of features needed in a CRM approach at large scales. This model also has the advantage that the numerical procedure developed in the next section can be analyzed explicitly in these important examples.

Under these conditions, it is well known (10, 11) that the equations in Eq. 10 reduce to a barotropic equation and an infinite number of decoupled shallow water equations,

$$\begin{aligned} \frac{\partial \vec{v}_H^q}{\partial t} + y \vec{v}_H^{q\perp} + c_q \nabla_H P^q &= 0 \\ \frac{\partial P^q}{\partial t} + c_q \text{div} \vec{v}_H^q &= \frac{1}{c_q} S_q(x, y, t), \end{aligned} \quad [11]$$

where

$$c_q = \frac{\bar{N}}{\lambda_q}, \quad P^q = \frac{p}{c_q}, \quad q = 1, 2, \dots, \quad [12]$$

and  $\lambda_q, q = 1, 2, \dots$ , with  $0 < \lambda_1 < \lambda_2 < \lambda_3, \dots$ , are the vertical separation constants determined by the eigenvalue problem,

$$G_q''(z) = -\lambda_q^2 G_q(z), \quad 0 < z < H, \quad G_q'(z) = 0, \quad z = 0, H, \quad [13]$$

with orthonormal eigenmodes,  $G_q(z)$ . The units of space and time in Eq. 10 have been nondimensionalized so that  $\beta = 1$  and so that the speed of the second baroclinic mode  $c_2 = (\bar{N}/\lambda_2)$ , satisfies,  $c_2 = 1$ . Thus, in nondimensional units, the wave speeds  $c_q$  associated with the other baroclinic modes are given by

$$c_q = \frac{\lambda_2}{\lambda_q}, \quad q = 1, 2, 3, \dots \quad [14]$$

The rationale for this choice of nondimensionalization rests in the fact that a typical value of  $c_2$  is 25 m/s (6), and it is desirable to resolve by a numerical strategy both the dry equatorial gravity waves with the speed, 50 m/s, and also the much slower convectively coupled waves (3, 5, 6) with a nearly Kelvin-wave structure with speeds of roughly 12 to 15 m/s (3, 5, 6). Of course, this choice is somewhat arbitrary and can be tuned conveniently from other considerations. The source terms,  $S_q(x, y, t)$ , in Eq. 11, are expansion coefficients of the general source  $S(x, y, z, t)$  in terms of the orthonormal eigenmodes,  $G_q(z)$ . The barotropic equation also has a source term determined by the vertical average of  $S$ . For simplicity in exposition, the barotropic mode contribution to Eq. 10 is omitted in the discussion here, because it can be treated separately in a different fashion.

### A Low-Order Meridional Truncation Strategy for Numerical Modeling

Here a general meridional truncation strategy is formulated for a general system of equations for a vector quantity,  $u$ ,

$$\frac{\partial u}{\partial t} + A_1(u)u_x + A_2(u)u_z + B(u)u_y + yLu = S(x, z, t, u), \quad [15]$$

where  $A_1(u), A_2(u), B(u)$  are matrix-valued nonlinear functions, and  $L$  is a constant matrix. In the example of the linearized primitive equations from Eq. 10, the state vector  $u$  represents all the variables,  $\hat{v}_H, w, B$ , and also  $p$ .

Given  $N$ , consider the approximate solution to Eq. 15 defined through the meridional grid levels  $y_j, j = 1, \dots, N$  associated with Gauss-Hermite quadrature, i.e.,

$$u_j(x, z, t) \cong u(x, z, y_j, t), \quad j = 1, \dots, N. \quad [16]$$

Recall the operation  $P_N$  defined in Eq. 8, which involves projection on the first  $N$ , parabolic cylinder functions. The Galerkin-collocation approximation to Eq. 15 involves the approximation

$$(B(u)u_y)(x, y_j, z, t) \cong B(u_j(x, z, t)) \left( P_N \frac{\partial}{\partial y} P_N u \right) (x, y_j, z, t) \\ (yLu)(x, y_j, z, t) \cong (P_N y L P_N u)(x, y_j, z, t). \quad [17]$$

For the moment, a precise definition of the operators on the right-hand side of Eq. 17 is postponed. With the approximations in Eqs. 16 and 17, the solution of Eq. 15 is replaced by the following approximation involving  $N$ -levels in  $y$ .

### The Meridional Truncation Equations

$$\frac{\partial u_j}{\partial t} + A_1(u_j) \frac{\partial u_j}{\partial x} + A_2(u_j) \frac{\partial u_j}{\partial z} + P_N (y L P_N u)(y_j, t) \\ + B(u_j) \left( P_N \frac{\partial}{\partial y} P_N u \right) (y_j, t) = S(x, y_j, t, u_j) \\ \text{for } j = 1, \dots, N. \quad [18]$$

Provided that the operators  $P_N (y L P_N)$  and  $P_N (\partial/\partial y) P_N$  can be computed efficiently, then the above equations are a meridional truncation of the equations in Eq. 15, which involves  $N$ -equations in the two  $(x, z)$  space variables alone, which are weakly coupled through these operators.

The operator  $P_N (\partial/\partial y) P_N u$  is defined as follows. Given the values,  $u(x, y_j, z, t)$ , from Eq. 9,  $P_N u$  is defined by

$$P_N u = \sum_{l=0}^{N-1} \tilde{u}_l \varphi_l(y) \\ \tilde{u}_l = \sum_{j=1}^N u(x, y_j, z, t) \varphi_l(y_j) \bar{H}_j. \quad [19]$$

With the properties in Eq. 3, one calculates

$$P_N \frac{\partial}{\partial y} P_N u = P_N \sum_{l=0}^{N-1} \frac{1}{2} \tilde{u}_l (L_+ + L_-) \varphi_l(y) \\ = P_N \sum_{l=0}^{N-1} \frac{1}{\sqrt{2}} \tilde{u}_l (l^{1/2} \varphi_{l-1}(y) - (l+1)^{1/2} \varphi_{l+1}(y)) \\ = \sum_{l=0}^{N-1} \frac{1}{\sqrt{2}} (\tilde{u}_{l+1} (l+1)^{1/2} - \tilde{u}_{l-1} l^{1/2}) \varphi_l(y). \quad [20]$$

Thus, the explicit formula is obtained,

$$\left( P_N \frac{\partial}{\partial y} P_N u \right) (y_j) = \sum_{l=0}^{N-1} \frac{1}{\sqrt{2}} (\tilde{u}_{l+1} (l+1)^{1/2} - \tilde{u}_{l-1} l^{1/2}) \varphi_l(y_j). \quad [21]$$

A similar calculation shows that

$$(P_N y L P_N u)(y_j) = \sum_{l=0}^{N-1} \frac{L}{\sqrt{2}} (\tilde{u}_{l+1} (l+1)^{1/2} + \tilde{u}_{l-1} l^{1/2}) \varphi_l(y_j). \quad [22]$$

It is worthwhile mentioning that from Eq. 20 in terms of the discrete Hermite coefficients,  $\tilde{u}_l, 0 \leq l \leq N-1$ , the operator  $P_N (\partial/\partial y) P_N$  is a skew-symmetric tridiagonal matrix with the form

$$\frac{\partial}{\partial y} P_N \underset{\text{Def.}}{=} \frac{\partial}{\partial y} P_N \\ = \frac{1}{\sqrt{2}} \begin{pmatrix} 0, & 1, & & & & & \\ -1, & 0, & 2^{1/2}, & & & & \circ \\ & -2^{1/2}, & 0, & 3^{1/2}, & & & \\ \circ & & & \ddots & & & \ddots \\ & & & & \ddots & & \ddots \\ & & & & & & (N-1)^{1/2} \\ & & & & & & - (N-1)^{1/2} & 0 \end{pmatrix}. \quad [23]$$

Similarly, from Eq. 22, the operator  $P_N y P_N$  is the symmetric tridiagonal matrix,

$$\hat{y}_N \underset{\text{Def.}}{=} P_N y P_N \\ = \frac{1}{\sqrt{2}} \begin{pmatrix} 0, & 1, & & & & & \\ 1, & 0, & 2^{1/2}, & & & & \circ \\ & 2^{1/2}, & 0, & 3^{1/2}, & & & \\ \circ & & & \ddots & & & \ddots \\ & & & & \ddots & & \ddots \\ & & & & & & (N-1)^{1/2} \\ & & & & & & (N-1)^{1/2} & 0 \end{pmatrix}. \quad [24]$$

With  $\tilde{u}_l$  defined from Eq. 19, the formulas in Eqs. 21 and 22 involve  $O(N^2)$  explicit matrix multiplications to generate the operators  $P_N (\partial/\partial y) P_N u$  and  $P_N y L P_N u$  at the  $y$ -levels  $y_j$  for  $j = 1, \dots, N$  and utilize only local operations for fixed  $x, z, t$ . For fixed  $N$ , these matrices can be precomputed and called for use in the algorithm. For moderate values of  $N$  such as  $N = 3, 4, 5$ , which are sufficient to capture the large-scale symmetric and antisymmetric equatorially trapped Kelvin, Yanai, and Rossby waves, these approximations are routine to implement directly and are completely local in  $(x, z)$ , because they involve processing of the meridional levels,  $u_j, j = 1, \dots, N$  for fixed  $(x, z, t)$ .

There is little physical interest in using such expansions for large values of  $N$ , because the equatorial waves with large  $N$  that are significantly less trapped in the equatorial wave guide are not observed, and instead nontrivial connections to midlatitude dynamics dominate. The approximations in  $y$  developed here are akin to the pseudospectral approximations with Fourier modes familiar to the reader (15). An important difference is that no fast Fourier transform is known for the operations in Eqs. 19, 21, and 22 to reduce the operation count for large  $N$ . This is irrelevant for the developments presented here, where it is

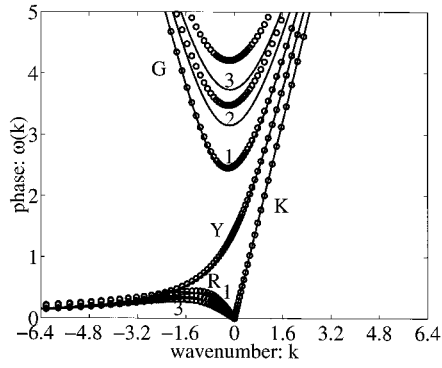


Fig. 1. Dispersion relations for  $c_q = 2$  and  $N = 5$ . Solid exact solution; circles numerical solution.

suggested that these models should be utilized only with small values of  $N$  to capture physically significant phenomena. The basic Galerkin approximation needs to be supplemented by a discrete radiation condition to not excite spurious large-scale modes that depend on  $N$  but are not equatorially trapped. Below, such a discrete radiation condition is described for the linearized equatorial primitive equations in the process of analyzing the basic algorithm presented above.

#### Application to the Linearized Equatorial Primitive Equations

If the basic meridional truncation strategy in Eq. 18 is applied to Eq. 10, by utilizing the same vertical structure equations in Eq. 13, the following approximations for the shallow water equations in Eq. 11 emerge:

$$\begin{aligned} \frac{\partial p_j}{\partial t} + c_q \frac{\partial u_j}{\partial x} + c_q P_N \frac{\partial}{\partial y} P_N v_j &= 0 \\ \frac{\partial u_j}{\partial t} + c_q \frac{\partial p_j}{\partial x} - P_N y P_N v_j &= 0 \\ \frac{\partial v_j}{\partial t} + c_q P_N \frac{\partial}{\partial y} P_N p_j + P_N y P_N u_j &= 0 \end{aligned} \quad \text{for } j = 1, \dots, N. \quad [25]$$

In Eq. 25,  $\vec{v}_H = (u, v)$  and the superscripts denoting the  $q$ th baroclinic mode have been dropped; the reader should note from Eqs. 19–24 that all  $N$  of the  $y$ -level values  $v_j$  are coupled in Eq. 25. Here the source terms,  $S_q$ , are ignored for simplicity in exposition. To show that an explicit analysis is possible, it is useful to introduce the vectors

$$\begin{aligned} \vec{w}_j &= (p_j, u_j, v_j), \quad j = 1, \dots, N \\ W &= (\vec{w}_1, \dots, \vec{w}_N) \\ \vec{W} &= (\vec{W}_0, \dots, \vec{W}_{N-1}) \\ \vec{W}_l &= \sum_{j=1}^N \vec{w}_j \varphi_j(y_j) \vec{H}_j, \quad l = 0, 1, \dots, N-1. \end{aligned} \quad [26]$$

and the  $3N \times 3N$  symmetric matrix,  $A$ , defined by

$$(A\vec{W})_j = \begin{pmatrix} 0, & c_q, & 0 \\ c_q, & 0, & 0 \\ 0, & 0, & 0 \end{pmatrix} \vec{W}_j \quad [27]$$

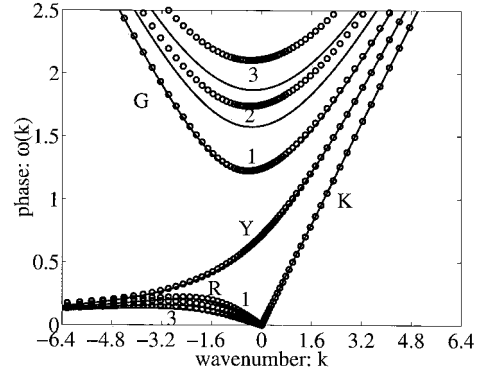


Fig. 2. Dispersion relations for  $c_q = 1/2$  and  $N = 5$ . Solid exact solution; circles numerical solution.

with  $\vec{W}_j = (\vec{p}_j, \vec{u}_j, \vec{v}_j)$ . With the explicit matrices in Eqs. 23 and 24 and Eqs. 26 and 27, the meridional truncated approximation in Eq. 25 becomes the constant coefficient equation for the Hermite coefficients,  $\vec{W}$ , given by

$$\frac{\partial \vec{W}}{\partial t} + A \frac{\partial \vec{W}}{\partial x} + B \vec{W} = 0, \quad [28]$$

where  $B$  is the skew-symmetric  $3N \times 3N$  matrix given explicitly by its action on  $(\vec{p}, \vec{u}, \vec{v})$  by

$$B = \begin{pmatrix} 0, & 0, & c_q \frac{\partial}{\partial \hat{y}_N} \\ 0, & 0, & -\hat{y}_N \\ c_q \frac{\partial}{\partial \hat{y}_N}, & \hat{y}_N, & 0 \end{pmatrix}. \quad [29]$$

Recall from Eqs. 23 and 24 that  $\partial/\partial \hat{y}_N$  is skew-symmetric, whereas  $\hat{y}_N$  is symmetric, so that  $B$  is necessarily an explicit skew-symmetric matrix. Thus, in terms of the discrete Hermite coefficients,  $\vec{W}_j$ , the meridional truncation approximation for the linearized primitive equations has the form in Eq. 28 for any of the higher baroclinic modes with  $A$  a symmetric matrix and  $B$  a skew-symmetric matrix. This has two important implications: first, the meridional truncation strategy is a linearly stable numerical procedure because

$$\sum_{j=0}^{N-1} \frac{1}{2} \int (\vec{u}_j^2 + \vec{v}_j^2 + \vec{p}_j^2) dx = \frac{1}{2} \int ((u, u)_N + (v, v)_N + (p, p)_N) dx \quad [30]$$

is conserved in time. Secondly, because  $A$  is symmetric and  $B$  is skew-symmetric, Eq. 28 is a dispersive wave equation so that the dispersion relations and corresponding eigenvectors for Eq. 28 can be calculated and compared with those for the equatorial shallow water equations in Eq. 11. The analysis presented below reveals the need for an additional discrete radiation condition to supplement the basic algorithm.

#### Spurious Modes and a Discrete Radiation Condition

With the variables

$$q = p + u, \quad r = p - u, \quad [31]$$

and the corresponding discrete Hermite expansion coefficients,  $\vec{q}_j, \vec{r}_j, \vec{v}_j$ , the dispersion wave system from Eq. 28 above can be rewritten as the coupled equations,



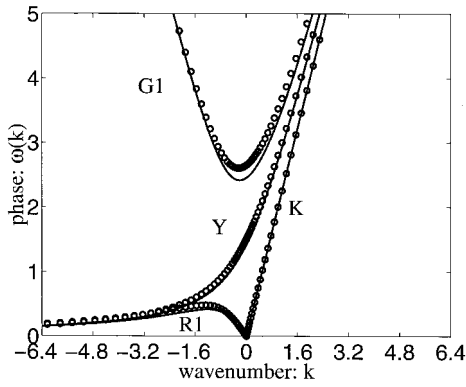


Fig. 3. Dispersion relations for  $c_q = 2$  and  $N = 3$ . Solid exact solution; circles numerical solution.

$$\begin{aligned} \frac{\partial \tilde{q}_j}{\partial t} + c_q \frac{\partial \tilde{q}_j}{\partial x} + \frac{1}{\sqrt{2}}(-c_q + 1)j^{1/2}\tilde{v}_{j-1} \\ + (c_q - 1)(j + 1)^{1/2}\tilde{v}_{j+1} = 0 \\ \frac{\partial \tilde{r}_j}{\partial t} - c_q \frac{\partial \tilde{r}_j}{\partial x} + \frac{1}{\sqrt{2}}(-c_q - 1)j^{1/2}\tilde{v}_{j-1} + (c_q + 1)(j + 1)^{1/2}\tilde{v}_{j+1} = 0 \\ \frac{\partial \tilde{v}_j}{\partial t} + \frac{1}{2\sqrt{2}}(-c_q - 1)j^{1/2}\tilde{q}_{j-1} \\ + (c_q + 1)(j + 1)^{1/2}\tilde{q}_{j+1} - (c_q + 1)j^{1/2}\tilde{r}_{j-1} \\ + (c_q - 1)(j + 1)^{1/2}\tilde{r}_{j+1} = 0, j = 0, 1, \dots, N - 1, \quad [32] \end{aligned}$$

with the convention  $\tilde{q}_j = \tilde{r}_j = \tilde{v}_j = 0, j = -1, N$ . For the simplest case with  $c_q = 1$ ,  $\tilde{r}_{N-1}$ ,  $\tilde{v}_{N-1}$ , and  $\tilde{r}_{N-2}$  solve the equations

$$\begin{aligned} \frac{\partial \tilde{r}_{N-1}}{\partial t} - \frac{\partial \tilde{r}_{N-1}}{\partial x} = 0 \\ \frac{\partial \tilde{r}_{N-2}}{\partial t} - \frac{\partial \tilde{r}_{N-2}}{\partial x} + \sqrt{2}(N - 1)^{1/2}\tilde{v}_{N-1} = 0 \\ \frac{\partial \tilde{v}_{N-1}}{\partial t} - \frac{1}{\sqrt{2}}(N - 1)^{1/2}\tilde{r}_{N-2} = 0. \quad [33] \end{aligned}$$

The first equation yields a completely spurious westward propagating “Kelvin-like” wave with a meridional structure strongly

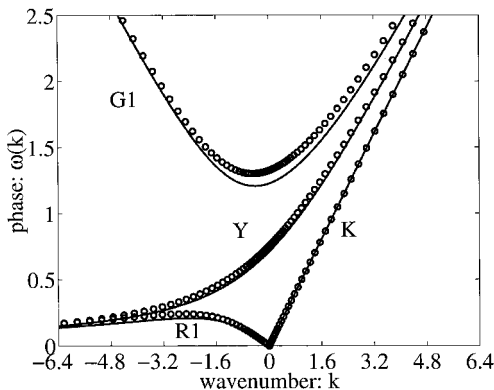


Fig. 4. Dispersion relations for  $c_q = 1/2$  and  $N = 3$ . Solid exact solution; circles numerical solution.

Table 1. Mean square relative error over the first 30 wave numbers in the dispersion relation

Wave	$N$	$c_q = 2$	$c_q = 1/2$	$c_q = 1/4$
Kelvin	3	0	0	0
Yanai		0.0130	0.0280	0.1562
Rosby ( $M = 1$ )		0.1805	0.1650	0.5215
Gravity ( $M = 1$ )		0.0193	0.0402	0.2146
Kelvin	4	0	0	0
Yanai		0.0057	0.0052	0.0768
Rosby ( $M = 1$ )		0.1886	0.1650	0.5215
Gravity ( $M = 1$ )		0.0193	0.0402	0.2146
Rosby ( $M = 2$ )		0.1769	0.1935	0.2281
Gravity ( $M = 2$ )		0.0342	0.0646	0.3091
Kelvin	5	0	0	0
Yanai		0.0064	0.0052	0.0768
Rosby ( $M = 1$ )		0.1670	0.0987	0.6201
Gravity ( $M = 1$ )		0.0037	0.0078	0.0943
Rosby ( $M = 2$ )		0.1769	0.1935	0.2281
Gravity ( $M = 2$ )		0.0342	0.1935	0.3091
Rosby ( $M = 3$ )		0.1355	0.1565	0.0609
Gravity ( $M = 3$ )		0.0501	0.0876	0.3832

dependent on  $N$ , whereas the second two equations yield spurious analogues of the Yanai waves with completely incorrect phases. On the other hand, for  $N \geq 2$  and  $c_q = 1$ , the approximation has the attractive feature that it exactly reproduces the equatorial Kelvin wave, Yanai wave, and all equatorial Rossby and gravity waves of index  $M$  with  $1 \leq M \leq N - 2$  together with their dispersion relations (10). These facts motivate the discrete radiation conditions for general solutions of the linearized equatorial primitive equations for  $N$ -meridional discrete levels,

$$\tilde{r}_{N-1}(x, z, t) = \tilde{r}_{N-2}(x, z, t) = \tilde{v}_{N-1}(x, z, t) \equiv 0, \quad [34]$$

with the corresponding condition imposed on the source terms,  $S(x, y, z, t)$ , which supplement the basic algorithm in Eq. 18 involving meridional truncation. Of course, these discrete radiation conditions in Eq. 34 should be applied only after the barotropic components have been removed by a straightforward vertical average.

#### Error Analysis for the Approximation for $c_q \neq 1$

Because the algorithm exactly reproduces all the trapped equatorial waves with index  $M \leq N - 2$  for a given  $N$  with  $c_q = 1$ , it is obviously interesting to evaluate the errors in the algorithm for  $c_q \neq 1$  via the theoretical procedure sketched above. Below, such errors are reported for the values,  $c_q = 1/2$  and  $c_q = 2$ , which correspond to dimensional Kelvin wave speeds of 12.5 m/s and 50 m/s, according to the nondimensionalization described earlier. As a more severe test case, some results are also reported for  $c_q = 1/4$ , which corresponds to a Kelvin wave speed of 6.25 m/s. Also the errors are reported here for  $N = 3, 4, 5$  so that there are only three, four, or five meridional levels of truncation; the values of  $N = 4, 5$  are small but still allow for exact resolution by the numerical algorithm for  $c_q = 1$ , the Kelvin, Yanai, and  $M = 1, 2$  equatorial Rossby and gravity waves, which are part of the observational record (3). The case with three meridional levels,  $N = 3$ , is also interesting as a minimal model with Kelvin, Yanai, and symmetric,  $M = 1$ , Rossby and gravity waves.

In Figs. 1 and 2, the numerical dispersion relation for  $N = 5$  and  $c_q = 1/2, 2$ , respectively, are compared with the exact dispersion relation for the Kelvin, Yanai, and equatorial Rossby and gravity waves with  $M = 1, 2, 3$ . Clearly, the phases of the Kelvin wave are exact and the Yanai wave nearly so, with small phase errors in the Rossby waves and  $M = 1$  gravity wave, and

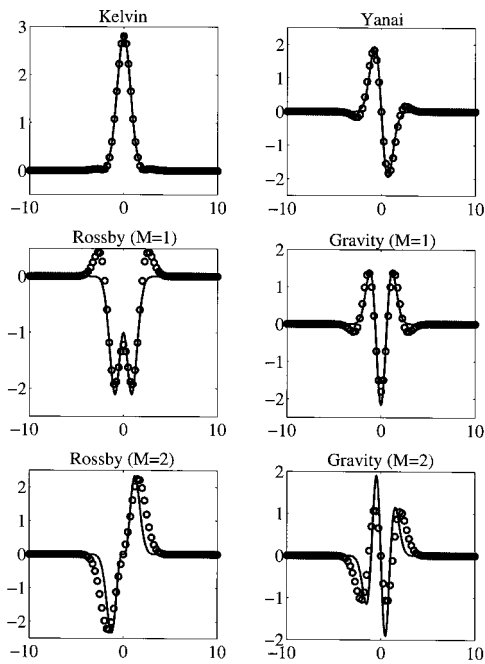


Fig. 5. Meridional structure of pressure for  $N = 5$ ,  $c_q = 1/2$  and wave number 5 ( $k = 5k_1$ ). Solid exact solution; circles numerical solution.

somewhat larger phase errors for the  $M = 2, 3$  gravity waves. Figs. 3 and 4 depict the same approximate dispersion relation with  $N = 3$ , with similar behavior.

To quantify these errors, recall that the fundamental wave number one for the earth is given by  $k_1 = 2\pi L_e/P$  with  $P = 40,000$  km and  $L_e = \sqrt{c/\beta}$  with  $c = 25$  m/s and  $\beta = 2\Omega/R$ ; thus,  $k_1 = 0.16$  and integer multiples of  $k_1$  denote the higher wave numbers. The first 30 wave numbers span scales down to 1,333 km. The mean square relative error over the first 30 wave numbers in the dispersion relation for  $N = 3, 4, 5$  and  $c_q = 2, 1/2, 1/4$  is presented in Table 1.

Note that the Kelvin wave has an exact dispersion relation, whereas the errors in the Yanai wave are small even for  $N = 3$  and  $c_q = 1/4$ . The largest relative errors in the dispersion relation occur consistently for the Rossby waves and are between 15 and 20% for  $c_q = 2, 1/2$ ; this could be anticipated, because the Rossby wave dispersion relation is nearly zero, so relative errors are exaggerated when compared with the excellent qualitative trends observed in Figs. 1–4 above.

How well does the algorithm resolve the spatial structure of the equatorial waves with the accurate dispersion relation described above for  $N = 3, 4, 5$ ? In Fig. 5, the meridional structure of pressure computed from the algorithm is compared with the exact answer for a representative wave number 5 and  $N = 5$  for the Kelvin, Yanai, and  $M = 1, 2$  Rossby and Gravity waves with  $c_q = 1/2$ . In Fig. 6, the same results are presented for wave

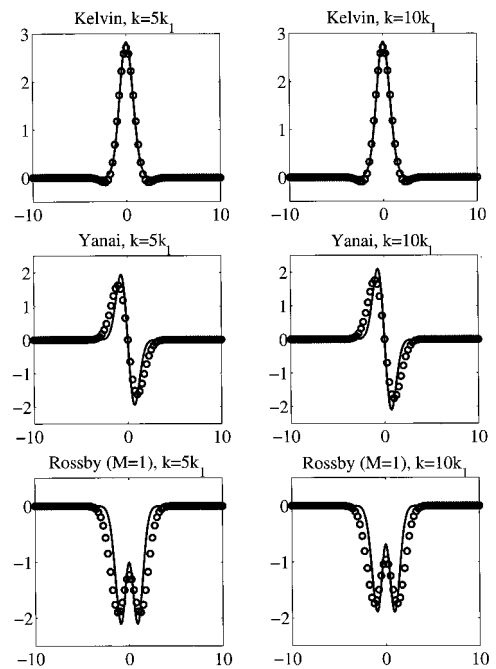


Fig. 6. Meridional structure of pressure  $N = 3$  and  $c_q = 1/2$  and wave numbers 5 and 10. Solid exact solution; circles numerical solution.

numbers 5 and 10 and  $N = 3$  for the Kelvin, Yanai, and  $M = 1$  equatorial Rossby wave. Considering the crudeness of the approximation, the qualitative discrepancies in the meridional structure are not very significant.

## Summary and Conclusion

A numerical algorithm designed specifically for efficient coupling of the equatorially trapped planetary waves with detailed two-dimensional cloud-resolving models (7–9) has been developed here. For the equatorial primitive equations, this algorithm amounts to the basic meridional truncation strategy developed in Eqs. 18, 21, and 22 combined with the readily implemented discrete radiation condition in Eq. 34 for the solution and heating sources. An explicit rigorous numerical analysis of the basic algorithm for the linearized equatorial primitive equations presented above reveals that only a small number of judiciously chosen meridional levels,  $N = 3, 4, 5$ , are needed to adequately represent a wide range of equatorially trapped waves, which form a significant part of the observational record (3). Detailed application of this basic algorithm for specific issues in tropical meteorology may be the subject of future research.

This research of A.M. is partially supported by grants from the National Science Foundation and the Office of Naval Research. B.K. is supported as a postdoctoral fellow through these grants.

1. Nakazawa, T. (1988) *J. Meteorol. Soc. Jpn.* **66**, 823–839.
2. Hendon, H. H. & Liebmann, B. (1994) *J. Geophys. Res. D* **99**, 8073–8083.
3. Wheeler, M. & Kiladis, G.N. (1999) *J. Atmos. Sci.* **56**, 374–399.
4. Emanuel, K. A. & Raymond, D. J., Eds. (1993) *The Representation of Cumulus Convection in Numerical Models, Meteorological Monographs*, Am. Met. Soc. Boston, MA, Vol. 48.
5. Majda, A. & Shefter, M. (2000) *J. Atmos. Sci.*, in press.
6. Majda, A. & Shefter, M. (2000) *J. Atmos. Sci.*, in press.
7. Grabowski, W. W., Wu, X. & Moncrieff, M. (1996) *J. Atmos. Sci.* **53**, 3684–3709.
8. Grabowski, W. W. *J. Atmos. Sci.* **55**, 3283–3298.
9. Grabowski, W. W. & Smolarkiewicz, P. K. (1999) *Physica D* **133**, 171–178.

10. Gill, A. E. (1982) *Atmosphere–Ocean Dynamics* (Academic, San Diego), Chap. 11.
11. Pedlosky, J. (1979) *Geophysical Fluid Dynamics* (Springer, New York).
12. Lebedev, N. N. (1972) *Special Functions and Their Applications* (Dover, New York).
13. Abramowitz, M. & Stegun, I. (1970) *Handbook of Mathematical Functions* (Dover, New York).
14. Ralston, A. & Rabinowitz, P. (1978) *A First Course in Numerical Analysis* (McGraw–Hill, New York).
15. Gottlieb, D. & Orszag, S. (1977) *Numerical Analysis of Spectral Methods* (Soc. Indust. Appl. Math., Philadelphia).